PROCEEDINGS OF SPIE

SPIEDigitalLibrary.org/conference-proceedings-of-spie

Gryphon M3 system: integration of MEMS for flight control

Adam Huang, Chris Folk, Chih-Ming Ho, Z. Liu, Wesley W. Chu, et al.

Adam Huang, Chris Folk, Chih-Ming Ho, Z. Liu, Wesley W. Chu, Yong Xu, Yu-Chong Tai, "Gryphon M3 system: integration of MEMS for flight control," Proc. SPIE 4559, MEMS Components and Applications for Industry, Automobiles, Aerospace, and Communication, (1 October 2001); doi: 10.1117/12.443022

SPIE.

Event: Micromachining and Microfabrication, 2001, San Francisco, CA, United States

Gryphon M^3 system: integration of MEMS for flight control

A. Huang*[a], C. Folk*[a], C.-M. Ho*[a], Z. Liu**[b], W.W. Chu**[b], Y. Xu***[c], Y.-C. Tai***[c]
[a]Dept. of Mechanical and Aerospace Engr., UCLA; [b]Dept. of Computer Science, UCLA; [c]Dept. of Electrical Engr., Caltech.

ABSTRACT

By using distributed arrays of micro-actuators as effectors, micro-sensors to detect the optimal actuation location, and microelectronics to provide close loop feedback decisions, a low power control system has been developed for controlling a UAV. Implementing the Microsensors, Microactuators, and Microelectronics leads to what is known as a M^3 (*M-cubic*) system. This project involves demonstrating the concept of using small actuators (~micron-millimeter scale) to provide large control forces for a large-scale system (~meter scale) through natural flow amplification phenomenon. This is theorized by using fluid separation phenomenon, vortex evolution, and vortex symmetry on a delta wing aircraft. By using MEMS actuators to control leading edge vortex separation and growth, a desired aerodynamic force can be produced about the aircraft for flight control. Consequently, a MEMS shear stress sensor array was developed for detecting the leading edge separation line where leading edge vortex flow separation occurs. By knowing the leading edge separation line, a closely coupled micro actuation from the effectors can cause the required separation that leads to vortex control. A robust and flexible balloon type actuator was developed using pneumatic pressure as the actuation force. Recently, efforts have started to address the most elusive problem of amplified distributed control (ADC) through data mining algorithms. Preliminary data mining results are promising and this part of the research is ongoing. All wind tunnel data used the baseline 56.5° sweepback delta wing with root chord of 31.75cm.

Keywords: MEMS, M^3 system, vortex flow, amplified distributed control (ADC), data mining

1. INTRODUCTION

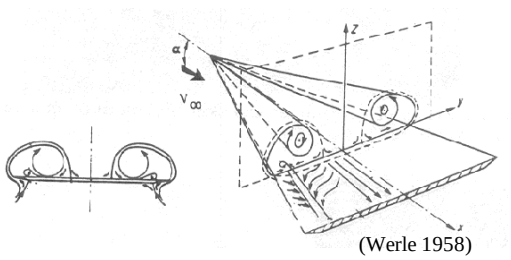

Fig. 1. Pairs of vortices above the delta wing

During the last decade, a MEMS-based technology for maneuvering delta-wing aircraft has been developed jointly by UCLA and Caltech. Instead of using conventional flaps to generate aerodynamic control, the feasibility of applying micromachined sensors and actuators for flight control was explored. The basic principle of using small length scale effectors to control large objects is through amplified distributed control (ADC). Basically, a natural amplification phenomenon is targeted and exploited to yield the desired global control effects. In the case of the delta wing, the pair of high suction primary vortices (Figure 1) was targeted for ADC through acknowledging the evolution of separated vortex flow that arise from flow separation lines near the leading edge of the delta wing. The resulting global structure of the primary vortices can be manipulated to provide control forces that are on the order of magnitude required for flight control at high angles of attack (>15° AoA; depending on sweepback angle)[1,2]. Like most MEMS projects, the MEMS technology is used as the enabling technology to provide the necessary sensors and/or actuators for customized requirements. In this project, a special aerospace sensor in the form of the flexible hot polysilicon shear stress sensor arrays was developed. The tailoring of thermal coefficient of resistance

* pohao@seas.ucla.edu; phone 1 310 825-8716; fax 1 310 825-1350; http://ho.seas.ucla.edu; UCLA Mechanical and Aerospace Engineering Department, Engineering I, RM 2124, 420 Westwood Plaza, Los Angeles, CA, USA, 90095; ** wwc@cs.ucla.edu; phone 1 310 825-2047; fax 1 310 825-2273; http://www.cobase.cs.ucla.edu; UCLA Computer Science Department, 3731H Boelter Hall, Los Angeles, CA, USA 90095-1596; *** yctai@touch.caltech.edu; phone 1 626 395-8317; fax 1 626 584-9104; http://touch.caltech.edu; Caltech Electrical Engineering Department, 1200 East California Boulevard, MS 136-93, Pasadena, CA, USA 91125

MEMS Components and Applications for Industry, Automobiles, Aerospace, and Communication,
Henry Helvajian, Siegfried W. Janson, Franz Lärmer, Editors, Proceedings of SPIE Vol. 4559 (2001)

(TCR) on silicon through doping results in a high bandwidth sensor that can be realized through appropriate feedback circuitry (constant temperature circuit) when compared with traditional metal filaments[3]. Using many MEMS specific process technologies, a hot filament surface sensor used for measuring shear stress have reached bandwidths higher than 100 kHz, while a free standing MEMS polysilicon hot wire have reached over 1 MHz. A flexible silicone membrane on copper substrate actuator has also been developed. This "bubble" actuator is actuated through pneumatic means and is capable of actuating more than 2mm and sustaining direct surface contacts (i.e., direct hand contact and handling)[4].

Following the development and testing of the MEMS sensors and actuators on the delta wing wind tunnel models, more appreciation was given to the complex problem of ADC. Most distributed control systems rely on the fact that each sensor and actuator group is simple and linear, and the advantage lies in the collective of the linear system. However, in the amplified distributed control scheme, the advantage of the collective of sensors and actuators also relies heavily on the individual group of local sensors and actuators. This is due to the amplified effects of the actuators and the nonlinear effect of the amplification phenomenon. Thus, the problem of providing an effective and accurate control scheme for a large distributed array of sensors and actuators for the delta wing is a difficult one. The main limitations are the non-linearity and the amplification sensitivity of the relationships describing the fluid-dynamics of vortex flow over a delta wing. In turn, the transfer function between the sensors, actuators, and flight control is extremely complex. In light of this, the adaptation of data mining methods is being pursued to combat this difficult yet generic problem that can be found in most complex physical interactions and natural ADCs. Unlike other methods of handling vast input/output variables such as neural networks, data mining also generates rules that governs the relationships, hence the ability to provide a quasi-transfer function of the complex physical phenomenon.

Researchers have developed data mining methods to classify large amounts of multivariable data for business and medical applications. Existing data mining methods, e.g., decision tree induction[5], rule derivation[6] or Bayesian learning[7], have been used on extremely large datasets with nonnumeric or categorical variables. However, data generated from scientific experiments are different from conventional datasets in the following aspects:

- Numerical variables involved are continuous and may take all distinct real numbers within valid ranges.
- Strong casual relationships exist among these numerical variables. The outcome of one dependent variable is often correlated with all the independent variables.

Therefore, the previous data mining methods are only suitable to business-like applications such as product forecasting and cross-selling where categorical variables prevail. Experimental engineering applications that discover patterns from experimental data require different data mining techniques. Preliminary data mining results using modified codes to handle real number vectors and actual wind tunnel results have been obtained. Predictions of limited MEMS actuator control and wind tunnel aerodynamic loading in the rolling axis are very promising. This part of the research is currently ongoing and, for the first time, it will extend into the unsteady motion of the wind tunnel model with MEMS sensors and actuators.

2. MECHANISM

2.1 Vortex lift and control

The rationale for the novel aerodynamic control concept is based on vortex control and amplified distributed control. Typical highly swept aircraft (i.e., delta wings) have a pair of symmetric vortices separating from the leading edge and convects down the wing (Figure 1). Each leading-edge vortex contributes a significant portion of lift to the delta wing. At high angles of attack, the lift force generated by these two leading-edge vortices can be as high as 40% for slender delta wings[8,9]. Numerous researches have shown that the genesis location of these vortices is very important to the characteristics of the resulting large primary vortices. Albeit the leading-edge vortex evolves into a large structure, its origin is quite compatible with the MEMS actuator length scale, hence the amplified distributed control. By controlling the evolution, convection vector, and the strength of these vortices with micro devices, desired aerodynamics loads can be elicited by appropriate spatial actuation. In effect, all six components of forces about an aircraft can be controlled; rolling, yawing, and pitching moments and drag, lift, and side forces of both positive and negative magnitudes. Figure 2 shows two possible vortex manipulation results with a MEMS actuator at the leading edge in comparison to no actuation. Figure 2 is taken with smoke particle flow visualization with the camera viewing head on toward the front of the wind tunnel model.

Fig. 2. Primary vortex shift in and shift out on the starboard side of the wind tunnel model.

In addition to other possible vortex movements such as lateral twist of the vortex core over the delta wing, recent computational fluid dynamic (CFD) analysis by Kaiden, et.al.[10] have shown that even more complicated flow patterns such as multiple vortex genesis, multiple vortex interactions, and primary vortex annihilation maybe be involved. Clearly it has validated the vortex shift control for flight vehicles and provided further insight into the next phase of this project using data mining.

2.1 Data mining principles

Large amount of data with numerous input/output vectors were collected during the wind tunnel testing of the MEMS sensors and actuators on the delta wing wind tunnel model. This is primarily due to the nature of the distributed array systems interacting with multidimensional and nonlinear systems. In order to efficiently sort out multidimensional relationships, data mining techniques was sought after rather than the more traditional vector limited graphical techniques. This represents a clear break with traditional experimental data analysis and may become an important new tool in the era of gathering more cross dimensional information than can be analyzed by traditional means. However, one should caution that data mining links raw data with raw data, and "expert" inputs before and after mining must be used to make raw numbers meaningful. This is done by associating physical meanings of the data at all times by casting attributes to each raw data vector. Based on the training sets obtained from experiments, two types of rules are mined: classification rules and association rules[11]. Classification rules are used to summarize the massive MEMS sensing/actuating data into a few variables, or often a single class variable. Association rules provide the correlation among the input variables and/or the output variables. A special type of association rule that captures the casual relationships between actuation and system output is called actuation rule. All these rules are in effect parts of the transfer functions that can be used for dynamic system control. Since the generated rules from data mining are not mutually exclusive, there may be many actuation rules that result in a desired output for a given environment. Strategies will be developed based on rule confidence, coverage and related association rules to select the rules for optimal actuation.

In distributed sensing and control applications, the number of sensors and variables used to derive rules from raw data are very large. As a result, traditional classification methods, such as a decision tree, either fail to complete the computation process or give poor classification results. These problems result because these methods are not able to handle multivariate inputs and/or process them efficiently. To remedy this problem, an efficient algorithm called Noah[12] has been developed to handle these situations. Noah performs an exhaustive search over all input variables to obtain the most useful classification rules. Noah is also tightly coupled with the database when searching for possible patterns. Therefore it is scalable to large data sets, unlike memory-bound algorithms that require all data manipulation to be done in the main memory. After the classification rules have been determined, the association rules will be mined to determine the relationship between the input/output vectors.

3. MEMS Devices

3.1 Flexible MEMS shear stress sensors

The flexible skin MEMS shear stress sensor was developed specifically for this project. The process flow is a merged process of bulk and thin film silicon micromachining. There are roughly four major iterations of design for this flexible skin MEMS shear stress sensor and is currently extremely mature. The latest process flow primarily focused on using Deep Reactive Ion Etching (DRIE) to perform the majority of the bulk silicon etching due to the high aspect ratio and silicon selectivity of such technique[13]. By using polyimide thin films as the flexible membrane, each shear stress sensor with the associated vacuum chamber underneath in a faceted manner (silicon islands) was fabricated and connected to yield a paper thin flexible shear stress sensor array. Furthermore, a Nickel/Gold layers was deposited using electroless plating on the backside, over evaporated aluminum, to allow a flip chip like bonding process with PC-boards (PCB). Figure 3 show the overall process flow of the flexible MEMS shear stress sensor array. Note that each silicon island is free standing and connected to the flexible polyimide thin film. The overall thickness of the film is ~80um with the silicon islands. Each silicon island is about 250x250 um in area which corresponds to the sensing resolution.

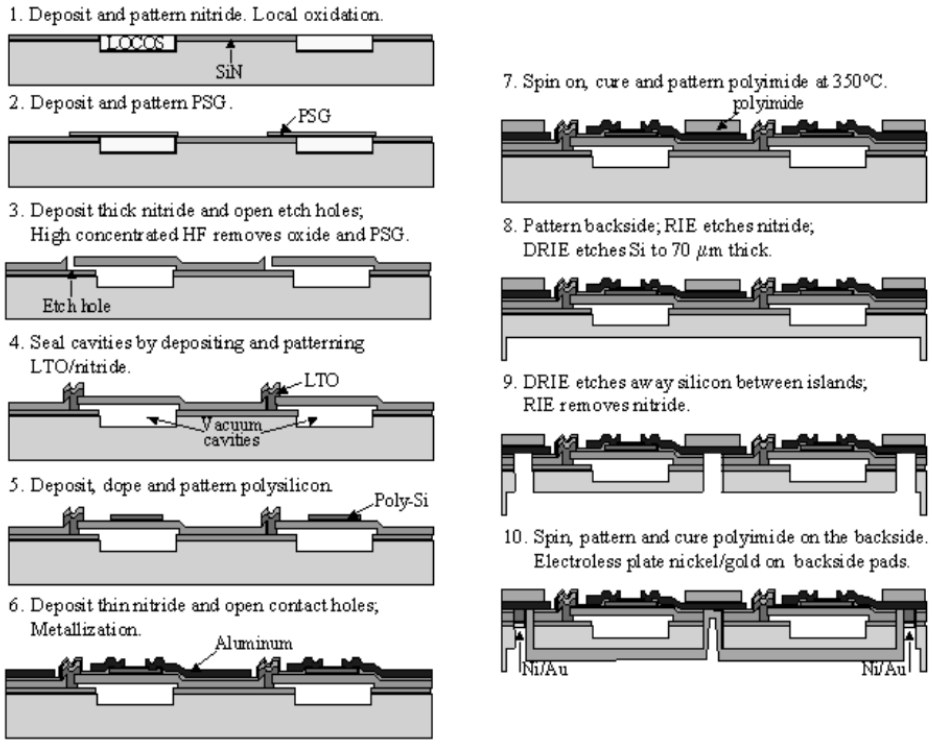

Fig. 3. Overall process flow of the flexible MEMS shear stress sensor array.

Figure 4 shows the latest generation of flexible shear stress sensor and the associated flexible Kapton® PCB. After "ironing" on the flexible MEMS shear stress skin to the PCB, the PCB is then wrapped on a small section of the leading edge radius. This sensor array contains 36 shear stress sensor elements coated with a thin layer of silicon nitride for maximum robustness in harsh environments. Further advances such as on sensor constant current drivers and signal multiplexers have been fabricated on a rigid silicon substrate equivalent of the flexible arrays. Wind tunnel tests have demonstrated the feasibility of effectively cutting down the wire leads dramatically (from shear stress sensor with associated wiring per element and off board constant current drivers to just a theoretical minimum of 4 contacts: 1)power, 2)ground, 3)serial address in, and 4)serial sensor data out).

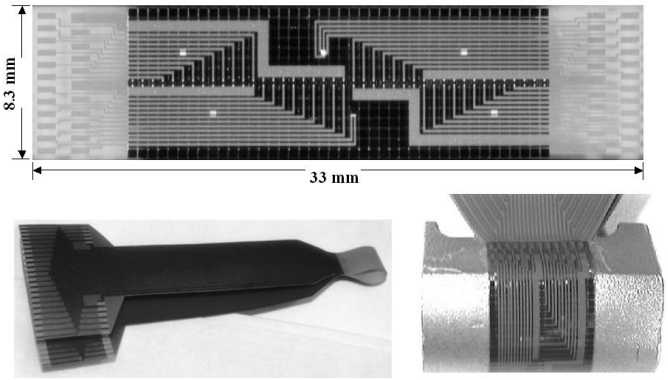

Fig. 4. Overall process flow of the flexible MEMS shear stress sensor array.

3.1 Flexible copper substrate silicone actuators

A new kind of MEMS actuator was also specifically developed for this project. Aerodynamic actuators that interact directly with the free stream have to endure rather harsh environments. A pneumatic actuator with silicone membrane on flexible metal substrates (copper) was developed so the actuators can also be used to wrap around smooth curvatures. This type of actuator is able to produce extremely large forces (>10mN) since the actuation principle relies on the pressure drop between the balloon membranes (>5 psi is easily achievable). At the same time actuation heights larger than 2mm was achieved. Figure 5 shows the relatively simple process flow of the "bubble" actuator and the final packaging of the actuator skin to the round cylindrical leading edge pieces of the wind tunnel model. Notice that the leading edge rods also provide the manifold for fluid passages to the actuators.

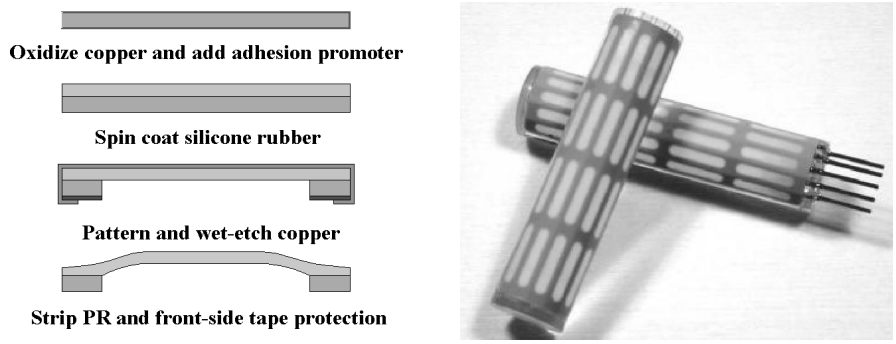

Fig. 5. Process flow and test articles of the flexible MEMS silicone actuators.

4. DATA

4.1 Leading edge shear stress level mapping

The leading edge separation data was gathered by using the flexible MEMS shear stress sensor arrays. The generation of the leading edge vortices actually arises from a line called the separation line. This is a highly curved line where surface flow (attached flow w.r.t aircraft skin) begins to separate and form the eventual vortex pairs. Since the local shear stress approaches the local minima near the separation line, this region of the leading edge is highly susceptible to small perturbation effects. This is the exact location where the amplification of the control phenomenon begins and ideally

this is the region where the MEMS actuators should be. Unfortunately, this line is not at a stationary position w.r.t the airfoil, but rather it is a highly complex function of many variables, such as AoA, Reynolds number, local and global wing geometry, and wing loading. In order to detect the separation line, the shear stress sensor was used to map out the entire shear level of the leading edge of the wind tunnel model. Since each sensor array is only roughly 1 cm wide, manual stepping of sensor location along the leading edge was used to map out along the length of it. Figure 6 shows the result of the shear stress mapping with the Y-axis showing the location of the sensor away from the apex (nose) of the wind tunnel model toward the wing tip. The X-axis shows the sensor location from the bottom of the wing (0 degrees) to the top of the wing (180 degrees). Figure 6 clearly shows the dark and white region of low and high shear stress respectively. It is also very clear that the separation line is not a very clearly defined line (the narrow light band between the dark and white region). Notice that at zero AoA, the wind tunnel model is parallel with the flow therefore no separation line and also yields near symmetric shear stress topography.

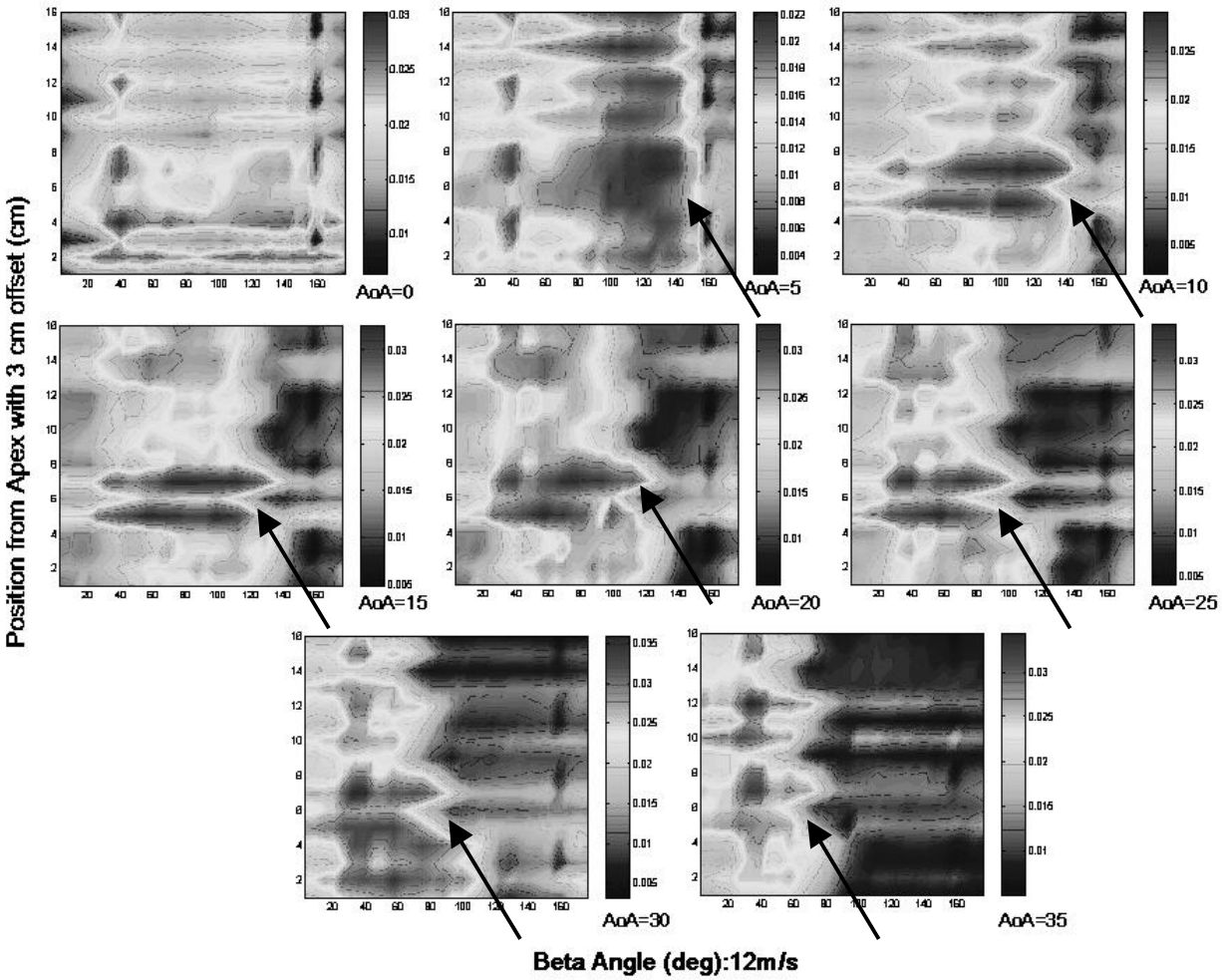

Fig. 6. Leading edge shear stress topography mapped from flexible shear stress sensor array. The arrow indicates the high to low shear stress transition, the separation line.

4.2 MEMS actuator control

Independent actuator tests performed in open loop fashion have consistently demonstrated the effectiveness of the vortex control scheme. A large amount of data collected were based on actuating a linear array of the silicone bubble actuators along the leading edge and recording the resulting forces and moments from a 6-component force balance. It was found for the wind tunnel model used, a 2mm actuation length is the most effective. This hints at the boundary layer being at

the similar magnitude and an effective length scale coupling was found. The actuation is digital and static (on or off), thus the actual flow interaction phenomenon is the surface boundary condition changed by the actuators which remodifies the separation line. Figure 7 shows the typical rolling moment coefficients created by the MEMS bubble actuation on the wind tunnel model. The actuation tests were conducted with about 4/5 of full span of the starboard leading edge fitted with a linear line of bubble actuators. The leading edge radius of the wind tunnel model is 6.35mm, while the pitch of the actuators are about 3mm, thus covering roughly 30 degrees of the leading edge (see Figure 5 for the actuator configuration). Again, the X-axis marks the beta angle, which is defined as 0 degrees for the lower surface (bottom of the wing) and 180 for the upper surface. Note that the overall range of the actuation is on the order of 0.01 rolling moment coefficient.

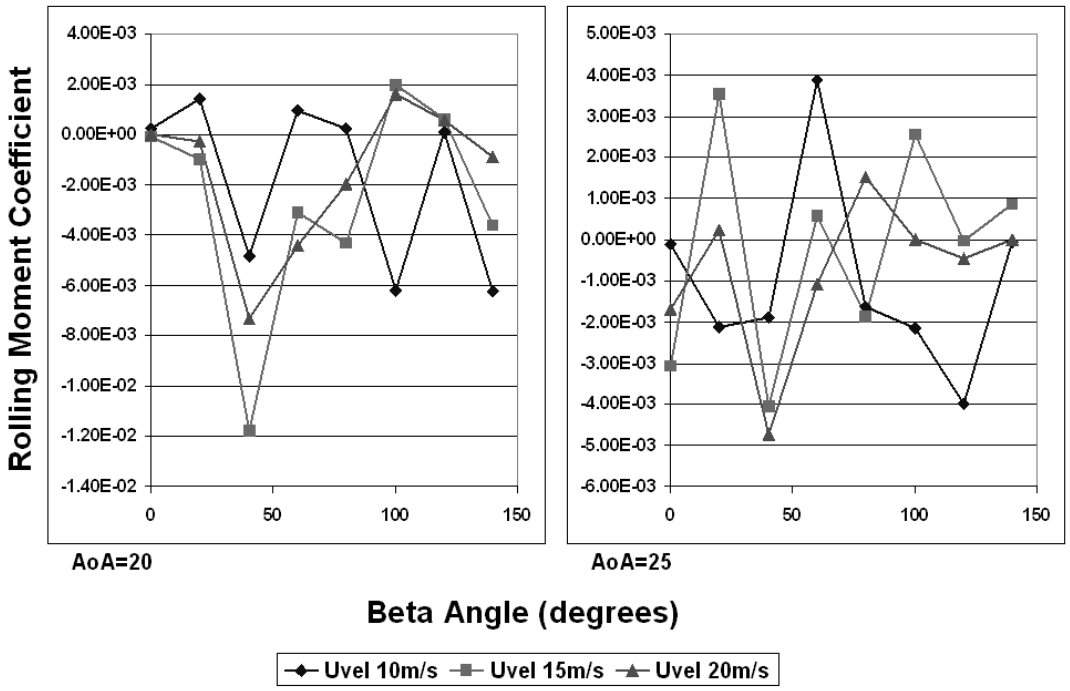

Fig. 7. Rolling moment coefficient created by the MEMS actuators for 20 and 25 degrees AoA at various velocities

5. RESULTS

5.1 Integration of MEMS sensors and actuators

After independent sensor and actuator tests, the two MEMS arrays were integrated to perform the integrated MEMS test with some simple separation line detection algorithms. A wind tunnel model was mounted with 2 strips of shear stress sensor arrays and full array of bubble actuators on the starboard side. The shear stress sensor is used to provide sampling points at defined location of the leading edge. By using two sampling points and a library of previously mapped out shear stress topographies, a simple actuation scheme was implemented to indicate the separation line. This is very crude, but provides the first time MEMS sensors and actuators function in a closed loop fashion to perform flight control. The control algorithm was able to select the proper location for actuation, however, since all test cases were done statically (the wind tunnel model being fixed), only a single space point is tested for each run. Figure 8 shows the wind tunnel model with the integrated sensor and actuator arrays. The left figure shows the starboard side of the model where the MEMS devices were installed. The sting mount contains a hollow shaft that allows wiring access to the sensors, actuator valves, and valve switching electronics mounted on the wind tunnel model. The right figure shows the setup without the top cover of the wind tunnel model.

Fig. 8. Integrated MEMS sensors and actuators mounted on the wind tunnel model.

5.2 MEMS actuator versus conventional flaps

It is of great interest to see exactly the effectiveness of the MEMS actuation scheme using vortex control versus conventional aerodynamic surfaces. Four conventional trailing edge flaps were added to the wind tunnel model and the normalization factor is scaled to compensate for the addition of wing surface areas. So far, only the rolling moment comparison was tested. It was found that at high angles of attack (> 15 degrees AoA) the MEMS bubble actuators were able to provide more than 50% of the outboard conventional flap surfaces. It should be noted that the MEMS actuation scheme is NOT optimized and an even higher rolling moment from the MEMS actuation should be achievable using distributed actuation (the comparison was against a linear MEMS actuation scheme). Figure 9 shows the plot of rolling moment coefficient of conventional aileron (45 degree deflection) versus the MEMS linear bubble actuators. The actuator length scale difference is 2 orders of magnitude, yet the loss of gain is only ~50% at high AoA.

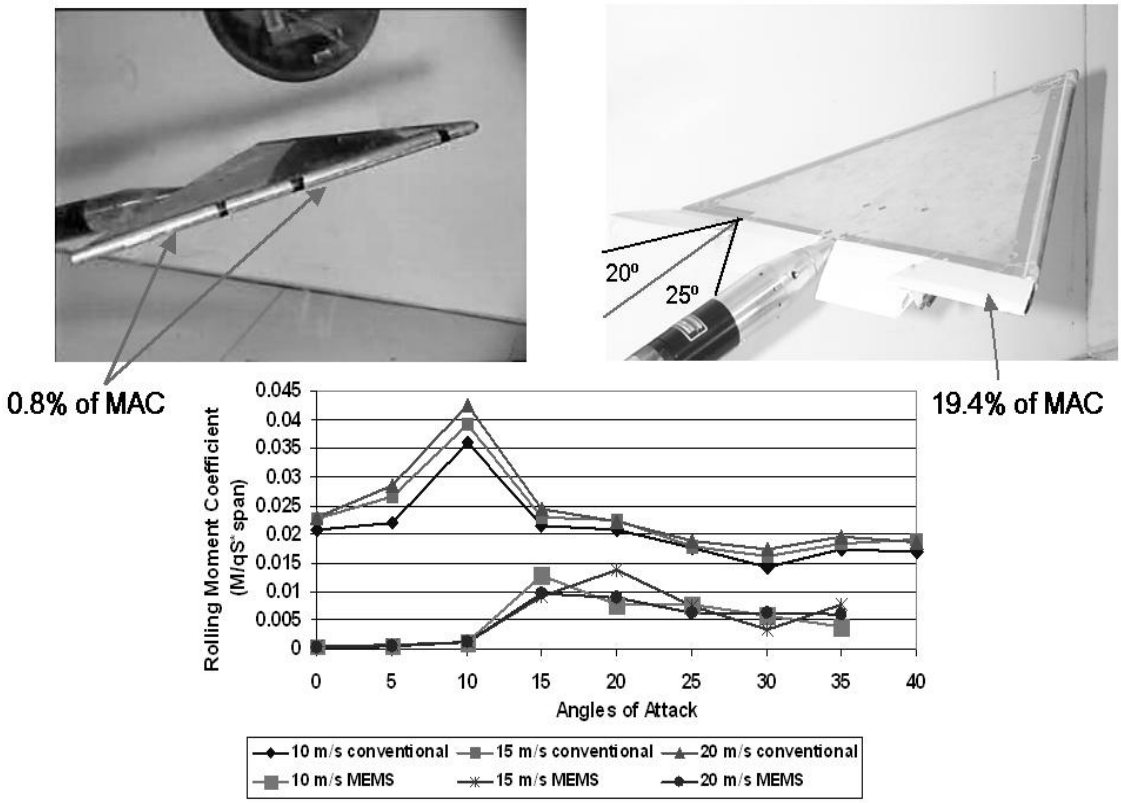

Fig. 9. MEMS actuators versus conventional flaps.

5.3 Preliminary Data mining results

With the current sensor/actuator integration, it is really not suitable for continuous unsteady tests due to lack of better data analysis capability. For example, the shear stress topography on figure 6 shows that the separation line is not a linear or simple curved line. It is highly nonlinear and rather sensitive to many variables. General attributes can be noticed; such as the averaged location of the separation line is an inverse function of the AoA (the higher the AOA, the lower the beta angle for the separation line). Albeit, this generalization is rather useless when it is imperative that the MEMS actuators need to be very near the separation line along the entire leading edge for effective control. Since from figure 7 it can be seen that the location of the actuation is very sensitive and large control force differences can be created by less than 20 degrees off from the optimum actuation location. In fact, sometimes the magnitude of the control force can change polarity when the actuation is just a few degrees off. Thus demonstrates the dilemma of the amplified distributed control systems. The natural amplification phenomena allows small devices to control large devices, but at the same time it is very elusive to dynamic systems since pin pointing the exact location for effective actuation becomes significantly harder.

The first step into tackling such a system is to derive the transfer function between the effectors and the affected. Solving multidimensional nonlinear systems is never an easy task, yet such trend of tackling extremely difficult nonlinear problems in the research field becomes more frequent recently. In this current project, data mining is being used to provide the nonlinear transfer function. The only set back with data mining is the required amount of experimental data that is needed, however, with today's automation and electronic data collection capabilities, it is a relatively easy task. Preliminary data mining has already demonstrated some very interesting capabilities. From figure 7, the rolling moment coefficients created by the MEMS actuators does not seems to create a generalized response. One hypothesis is that the effect is multivariable and multidimensional. Traditional graphical methods becomes increasingly hard to decipher when the dimensions on a graph reaches more than 4 vectors (x,y,z,t). Instead of manually looking for recognizable patterns through graphical means, data mining methods automatically identify statistically strong patterns embedded in input-output relationships. By grouping similar patterns together, the original data is greatly summarized with reduced dimensionality. Rules are then developed to create insight of the physical phenomenon and hopefully the much sought after nonlinear transfer function. This type of processing scales well when handling extremely large data collections and outperforms traditional statistical methods in terms of efficiency. By using data collected from other angles of attack and velocities, a preliminary rule generated by data mining indicated cross talking of the AoA and Velocity. Figure 10 shows normalized lines of different test cases with different multivariable conditions (i.e., different AoA and Velocity), yet the data mining software was able to generate an averaged trend based on derived rules. Although this is a relatively simple rule to generate, further progress of this project will be sought after in the unsteady region of flight control.

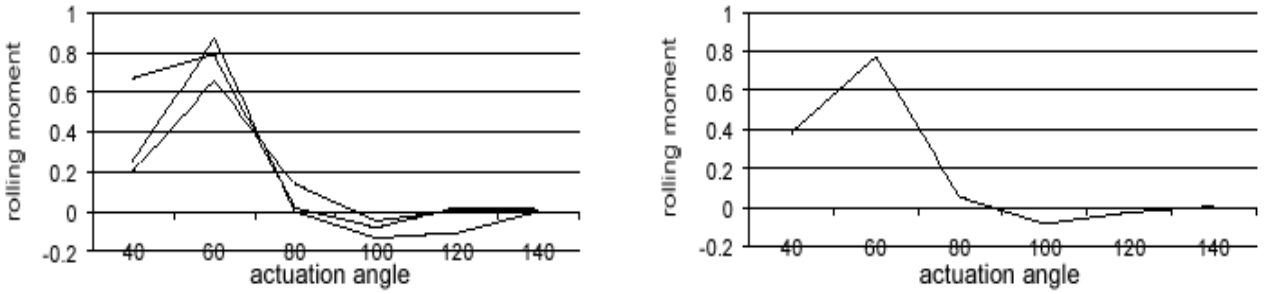

Fig. 10. Data mining results after clustering and pruning raw wind tunnel data(left). An average result is then generated from the derived rules (right).

6. CONCLUSION

After nearly a decade of research into vortex control on delta wing with MEMS devices, this project accomplished the feat fabricating the necessary MEMS devices (MEMS sensors and actuators) and supported the feasibility of using amplified distributed control for flight vehicle control. MEMS actuators developed have clearly demonstrated the capability of eliciting similar control forces on a wind tunnel model that uses conventional actuators that are over 2 orders of magnitude larger. MEMS shear stress sensors have demonstrated capability of sensing and mapping surface shear forces with great spatial resolution and temporal response. Currently, the project is gearing up for unsteady wind tunnel experiments in conjunction with data mining to obtain control laws/"rules" for unsteady flight control.

ACKNOWLEDGEMENT

The authors would like to thank the Defense Advanced Research Projects Agency (DARPA), the NASA DRYDEN Research Flight Center, and National Science Foundation (NSF) for the support of the projects. The authors would also like to thank numerous previous graduate students and other personnel involved in this project, specially noted is G.B. Lee who was the primary graduate student of the first phase of this project.

REFERENCES

1. G.B. Lee, S. Chiang, Y.C. Tai, T. Tsao, and C.M. Ho, " Robust vortex control of a delta wing using distributed MEMS actuators," *Journal of Aircraft* (2000).
2. A. Huang, C. Folk, C. Silva, B. Christensen, Y.F. Chen, G.B. Lee, M. Chen, S. Newbern, F. Jiang, C. Grosjean, C-M. Ho, and Y.-C. Tai, "Applications of MEMS devices to delta wing aircraft: From concept development to transonic flight test," AIAA, Reno, Nevada 01-0124, January, 2001.
3. J.B. Huang, F.K. Jiang, Y.C. Tai, and C.M. Ho. "A Micro-Electro-Mechanical-System-based thermal shear stress sensor with self-frequency compensation," *Meas. Sci. Technol*. 10(1999)687-696.
4. Huang, A., Ho, C.M., Jiang, F., and Tai, Y.C., "MEMS Transducers for Aerodynamics-A Paradigm Shift," AIAA 00-0249, Reno, Nevada, January, 2000.
5. M. Mehta, R. Agrawal, and J. Rissanen. SLIQ: A fast scalable classifier for data mining. In *Proc. of the 5th Int'l Conf. on Extending Database Technology (EDBT)*, Avignon, France, March 1996.
6. R. Agrawal, H. Mannila, R. Srikant, H. Toivonen, and A.I. Verkamo. Fast discovery of association rules. In U. M. Fayyad, G. Piatetsky-Shapiro, P. Smyth and R. Uthurusamy, editors, *Advances in Knowledge Discovery and Data Mining*, pages 399-421. AAAI/MIT Press, 1996.
7. C. Elkan. Boosting and naive bayesian learning. Technical report no cs97-557. Dept. of Computer Science and Engineering, UCSD, September 1997.
8. Polhamus, E.C. "Vortex Lift Research: Early Contributions and Some Current Challenges," *Vortex Flow Aerodynamics*, NASA CP2416. pp. 1-30.
9. Polhamus, E.C., "Predictions of Vortex-Lift Characteristics by a Leading-Edge-Suction Analogy," *Journal of Aircraft*, Vol. 8, No. 4, pp.193-199., Vol. 70, No. 5, pp. 420-456, 1971.
10. T. Kaiden, and Y. Nakamura, "Numerical Analysis of Aerodynamic Control by Micro-flap around Delta Wing," *19th AIAA Applied Aerodynamics Conference*, Anaheim, California, 01-2441.
Zhenyu Liu, Wesley W. Chu, Adam Huang, Chris Folk, Chih-Ming Ho
11. *"Mining Sequence Patterns from Wind Tunnel Experimental Data for Flight Control"*, Proc. 5th Pacific-Asia Conf. on Knowledge Discovery and Data Mining (PAKDD), Hong Kong, China, April 2001.
12. G. Giuffrida, W. W. Chu, and D. M. Hanssens. NOAH: An algorithm for mining classification rules from datasets with large attribute space. In *Proceedings of 12th International Conference on Extending Database (EDBT)*, Konsta, Germany, March 2000.
13. Jiang, F., Xu, Y., Weng, T., Han, Z., Tai, Y.C., Huang, A., Ho, C.M., and Newbern, S., "Flexible Sensor Skin for Aerodynamics Applications," MEMS-2000, Miyazaki, Japan, pp. 465-470, 2000.